Received: 5 January 2024 | Revised: 21 June 2024 | Accepted: 23 June 2024

DOI: 10.1002/rcm.9866

RESEARCH ARTICLE

Rapid Communications in Mass Spectrometry WILEY

Sulfur isotope analyses using 3× elemental analysis/isotope ratio mass spectrometry: Saving helium and energy while reducing analytical time and costs

Jorge E. Spangenberg | Alice Bosco-Santos

Institute of Earth Surface Dynamics (IDYST), University of Lausanne, Lausanne, Switzerland

Correspondence
Jorge E. Spangenberg, Institute of Earth Surface Dynamics, University of Lausanne, Geopolis Building, CH-1015 Lausanne, Switzerland.
Email: jorge.spangenberg@unil.ch

Funding information
University of Lausanne; Swiss National Science Foundation; Foundation Agassiz

Rationale: Helium (He) and energy shortages have caused price increases and reduced their availability. Using three combustion reactions per acquisition of carbon and nitrogen isotope ratios saves 50% He and energy during the elemental analysis/isotope ratio mass spectrometry (EA/IRMS). This approach needs to be tested for sulfur isotope ($\delta^{34}S$) analyses.

Methods: A new method to measure $\delta^{34}S$ in three sequential combustion reactions within one EA/IRMS acquisition was developed. The same material or blank samples could be used in the three reactions. After SO_2 was used, a N_2 purging method was employed to prolong the lifetime of the valves in the EA/IRMS interface. The 3×EA/IRMS was applied to measure $\delta^{34}S$ in precious samples, such as Ag_2S from acid-volatile and chromium-reducible sulfur extracted with a multiple-port setup.

Results: The 3×EA/IRMS-$\delta^{34}S$ method was validated with replicate analyses of international reference materials and laboratory standards with a wide range of mineralogical compositions and $\delta^{34}S$ values. The method provided a strategic advantage for the $\delta^{34}S$ measurements of small precious samples (measured between blanks). The accuracy and precision of the 3×EA/IRMS values effectively matched those obtained using conventional EA/IRMS, with good agreement between the mean ± SD values and the recommended values with their uncertainties.

Conclusions: Compared with the conventional EA/IRMS, the proposed method provides accurate and precise $\delta^{34}S$ measurements of the sulfate and sulfide samples while saving approximately 50% of He, energy, SO_2 reference gas, O_2, analysis time, and cost. Notably, 3×EA/IRMS can provide up to three $\delta^{34}S$ values unaffected by memory effects.

1 | INTRODUCTION

Helium (He) and energy are required for various scientific research and industrial applications. However, the global demands for He[1–4] and energy[5,6] are rapidly outpacing the supplies. This situation has triggered a steady increase in their prices, prompting the exploration of new technologies that are less reliant on these resources. An effective way to alleviate this problem is to optimize the application methods with high He and energy-demanding instrumentation, such as elemental analysis/isotope ratio mass spectrometry (EA/IRMS). This approach

would save He and electricity consumption, thereby alleviating costs for academic and industrial laboratories. Recently, modifications of the EA/IRMS acquisition methods, which would ensure a 50% savings in He, energy, analytical time, and costs, were proposed for carbon and nitrogen isotope ($\delta^{13}C$ and $\delta^{15}N$ values) analyses.[7] Here, we expand this development to the sulfur isotope ratio analyses.

The stable isotope ratios of sulfur ($\delta^{34}S$ values relative to Vienna Cañon Diablo Troilite [VCDT]) in sulfates and sulfides are remarkable tools for studying geochemical and biogeochemical cycles in ancient[8–12] and modern environments.[13–15] $\delta^{34}S$ is routinely measured using EA/IRMS[16,17] and, less frequently, multicollector inductively coupled plasma mass spectrometry (MC-ICP/MS).[18,19] The MC-ICP/MS system may use an Ar–He mixture as a carrier and ionization gas and consume less He than the EA/IRMS system, but it is a pricier technology and is not used widely.

In the prevailing EA/IRMS acquisition method, one strategy to reduce He and energy consumption while analyzing $\delta^{13}C$ and $\delta^{15}N$ involved a substantial reduction (i.e., 50%) in the analytical time per sample.[7] Initially featuring a single combustion, the optimized method incorporated two EA combustion reactions per single EA/IRMS acquisition.[20] This innovative approach pioneered for the EA/IRMS analyses of $\delta^{13}C$ in volatile liquid samples[20] stemmed from the need to minimize the residence time of the capsule with liquid volatile organic compounds in the sample drum and cavity of the pneumatic autosampler (i.e., AS-2000LS, Fisons Instruments, Milan, Italy) of the elemental analyzer. More recently, an improved method called 3×EA/IRMS[7] used three combustion reactions to measure carbon or nitrogen isotope ratios in triplicate for calibration, quality control standards, or samples. In practical terms, this approach can be used with three combustions of different standards or unknown materials without affecting the accuracy and precision of the measured isotopic ratios. The present study was intended to extend the application of 3×EA/IRMS for sulfur isotope analyses of sulfides and sulfates.

The incorporation of three capsule combustions within a single EA/IRMS acquisition for $\delta^{13}C$ or $\delta^{15}N$ analyses had no impact on the background signals (i.e., traces of *m/z* 44, 45, and 46 and *m/z* 28, 29, and 30 for the ions of CO_2 and N_2 gases; figure 1 in Spangenberg[7]) when compared to the conventional EA/IRMS acquisitions. Nevertheless, the application of 3×EA/IRMS for $\delta^{34}S$ measurement may pose potential challenges due to the "sticky" nature of the sulfur dioxide (SO_2) gas. This characteristic may lead to peak tailing, memory effects, and high background levels in the *m/z* 64 and 66 traces due to the carryover of residual gases from previous combustion reactions. These issues could result in isotopic discrepancies. The optimized EA and IRMS conditions would likely mitigate these challenges.

As an additional contribution, a simple technical setup is provided; this setup was designed by the first author at the University of Lausanne (UNIL) laboratories for purging the residual gases in the tubing and valves from the SO_2 reference gas cylinder to the continuous flow interface (i.e., ConFlo III), linking the elemental analyzer and the isotope ratio mass spectrometer. This connection enables the system to be purged with pure N_2 gas after SO_2 usage. This setup minimizes the build-up of residual SO_2 in the valves, tubing, connections, capillaries, and reference gas open split, increasing the lifetimes of the pressure regulators, valves, and gauges attached to the SO_2 gas cylinder and those within the ConFlo interface.

Finally, we present an example of sulfur isotope analysis of samples with a minimal amount of precious material using 3×EA/IRMS. We measured $\delta^{34}S$ of acid-volatile sulfur (AVS) and chromium-reducible sulfur (CRS-pyrite) between two blanks (i.e., empty capsules) and avoided sample wastage by potential sample tailing and memory effect. The AVS and CRS-pyrites were extracted from recent and ancient sediments using a setup that could simultaneously extract reduced sulfur species from multiple samples. We provide details on each part of this apparatus, including its dimensions, product names, and supplier part numbers.

2 | MATERIALS AND METHODS

2.1 | Materials

International reference materials (RMs) and laboratory standards (Table 1) were used to validate the 3×EA/IRMS procedure. Further evaluations of the robustness of the 3×EA/IRMS procedure were performed for $\delta^{34}S$ analyses of a wide range of sulfide minerals from different ore deposits provided by students and researchers at the Universities of Lausanne and Geneva. Some of these samples had been previously analyzed for $\delta^{34}S$ with conventional EA/IRMS. The CRS-pyrite was extracted from recent and ancient sediments, including sediments from Lake Joux in Canton Vaud, Switzerland (46.5863° N, 6.2616° E), and black shales from the 2.72 Ga Rio das Velhas greenstone belt in Minas Gerais, Brazil.[23] The sediment samples were freeze-dried at −50°C and <1 mbar for 48 h and homogenized with an agate mortar and pestle. The sedimentary rock samples were powdered in an agate mill ball and homogenized manually.

The consumables for the elemental analyses (described later) were purchased from Säntis Analytical (Teufen, Switzerland). Milli-Q purified water (MQW; 18.2 MΩ cm resistivity at 25°C) was obtained with a Direct-Q UV 3 Milipore system (Merck, Darmstadt, Germany). Nitrogen and He (both of 99.999% purity) and oxygen (99.998% purity) used in the EA/IRMS were purchased from Air Liquide/Carbagas (Lausanne, Switzerland). SO_2 (99.98% w/w purity, CAS No. 7446-09-5) in a 6.1 kg gas cylinder produced by Gerling Holz & Co. Handels GmbH (GHC; Hamburg, Germany) was obtained from Multigas (Domdidier, Switzerland). All the chemicals used for AVS and CRS extractions were high purity grade; they included chromium (III) chloride hexahydrate ($CrCl_3{\cdot}6H_2O$, ≥96.0%, CAS No. 10060-12-5), granulated zinc (Zn, 14–50 mesh ASTM, 0.3–1.5 mm particle sizes, CAS No. 7440-66-6), zinc acetate dihydrate ($Zn(CH_3CO_2)_3{\cdot}2H_2O$, ≥99.5%, CAS No. 5970-45-6), silver nitrate ($AgNO_3$, ≥99.8%, CAS No. 7761-88-8), ammonium hydroxide solution (28%–30% NH_3, CAS N 1336-21-6), and ethanol (C_2H_6O; ≥99.9%, CAS No. 64-17-5) and were obtained from Merck AG (Dietikon, Switzerland). Fuming hydrochloric acid (37% v/v with ≤0.0005% w/w sulfate and

TABLE 1 Sulfur isotope compositions of the international reference materials and laboratory standards obtained using conventional elemental analysis/isotope ratio mass spectrometry (EA/IRMS) and 3×EA/IRMS.

		$\delta^{34}S_{VCDT}$ (mUr)						
			EA/IRMS[b]		3×EA/IRMS (the three values)		3×EA/IRMS (2nd and 3rd values)	
Identifier	Material (chemical formula)	Accepted[a]	Average	SD (n)[c]	Average	SD (n)[c]	Average	SD (n)[c]
NBS 127	Barite ($BaSO_4$)	21.12 ± 0.22	21.05[b]	0.37 (14)	21.09	0.31 (12)	21.17	0.12 (8)
IAEA-SO-5	Barite ($BaSO_4$)	0.49 ± 0.11	0.53	0.16 (12)	0.54	0.24 (12)	0.46	0.10 (8)
IAEA-SO-6	Barite ($BaSO_4$)	−34.05 ± 0.08	−34.08	0.20 (12)	−34.06	0.46 (12)	−34.08	0.19 (8)
IAEA-S-4	Elemental sulfur (S)	16.90 ± 0.12	17.09[b]	0.18 (8)	16.84	0.20 (6)	16.90	0.20 (4)
IAEA-S-1[d]	Silver sulfide (Ag_2S)	−0.3	−0.32	0.21 (8)	−0.27	0.12 (6)	−0.19	0.05 (4)
IAEA-S-2	Silver sulfide (Ag_2S)	22.62 ± 0.16	22.56	0.15 (8)	22.54	0.24 (6)	22.68	0.12 (4)
IAEA-S-3	Silver sulfide (Ag_2S)	−32.49 ± 0.16	−32.58	0.26 (8)	−32.54	0.29 (6)	−32.53	0.24 (4)
NBS 122[e]	Sphalerite (ZnS)	0.18 ± 0.14	−0.01[b]	0.17 (10)	0.15	0.20 (6)	0.24	0.19 (4)
NBS 123[e]	Sphalerite (ZnS)	17.09 ± 0.32	17.22[b]	0.22 (10)	17.68	0.19 (6)	17.48	0.16 (4)
		17.44 ± 0.10						
UVA-sulfate	Synthetic barium sulfate	12.73 ± 0.21	12.66[b]	0.23 (15)[c]	12.63	0.30 (9)	12.77	0.11 (6)
Fx-sulfate	Synthetic barium sulfate	17.82 ± 0.22	17.86[b]	0.26 (10)	17.87	0.19 (9)	17.92	0.19 (6)
UNIL-PyE	Pyrite (FeS_2)	−6.72 ± 0.19	−6.69[b]	0.20 (14)	−6.76	0.31 (12)	−6.78	0.29 (8)
UNIL-cinnabar	Synthetic mercury sulfide (HgS)	15.82 ± 0.15	15.79[b]	0.14 (12)	15.74	0.33 (11)	15.87	0.23 (8)
Average				0.212		0.261		0.168
SD				0.061		0.086		0.066

Abbreviations: IAEA, International Atomic Energy Agency; NBS, National Bureau of Standards;SD, standard deviation; UNIL, University of Lausanne; UVA, University of Virginia.

[a]Values for the international reference materials (RMs) from Brand et al.[21] Values for the laboratory standards obtained using EA/IRMS measurements.[22]

[b]Values obtained using conventional EA/IRMS measurements[22]; otherwise, values obtained from quality control standards in sequences run during April 2022 and January 2023.

[c]Uncertainty values correspond to one SD (1-sigma) of n measurements.

[d]Primary Vienna Cañon Diablo Troilite (VCDT) reference with the exact value defining the $\delta^{34}S_{VCDT}$ scale.

[e]Discontinuous, possibly nonhomogeneous.[21]

≤0.0010% w/w sulfide, CAS No. 7647-01-0) was obtained from Carlo Erba, Val-de-Reuil, France. The following solutions were prepared for AVS and CRS extractions: 6 N HCl, 1.0 M $CrCl_3$, 0.6 N HCl, 25% v/v HCl, 0.2 M zinc acetate, and 0.1 M silver nitrate. An acidic 1.0 M $CrCl_2$ solution was prepared shortly before use by reacting a 1.0 M $CrCl_3$ solution with granulated zinc in a two-neck round-bottom flask (RBF) under N_2 flow until the solution color changed from green to dark blue, the characteristic color of the solution with a prevailing $CrCl_2$ concentration.

2.2 | Sulfur isotope analyses at the UNIL using EA/IRMS system

Sulfur isotope measurements in the UNIL were performed using EA/IRMS with a system composed of a Carlo Erba 1108 elemental analyzer equipped with an AS-200LS pneumatic autosampler (both from Fisons Instruments, Milan, Italy) connected to a Delta V Plus isotope ratio mass spectrometer via a ConFlo III interface (both from Thermo Fischer Scientific, Bremen, Germany), as described previously.[7,22]

The EA combustion/reduction reactor for the sulfur analyses consisted of a transparent quartz tube (450 mm length and 18 mm OD; from Säntis Analytical, Teufen, Switzerland, part no. SA46820070); this quartz tube was filled from the bottom to the top with 30 mm quartz wool (part no. SA990716B), followed by 90 mm reduced copper wires with 0.7 mm OD (part no. SA99060204), 40 mm quartz chips measuring 1–4 mm in size (part no. SA990715), and tungsten (VI) oxide granulates with a 12–35 mesh grain size (part no. SA990702) (Figure 1A). No quartz wool or quartz inserts were placed on the top of the reactor. The combustion gases were passed to a water trap consisting of a glass tube (11 mm length, 10 mm ID, 12 mm OD; part no. SA990740) filled with dried magnesium perchlorate ($Mg(ClO_4)_2$, part no. SA990712) with a He flow of 80 mL/min. The SO_2 in the dried combustion gases was separated in a polytetrafluoroethylene (PTFE) gas chromatography (GC) column (80 cm length, 4 mm ID, 12 mm OD) filled with Hayesep Q 80–100 mesh (part no. SA99073) and carried into the ConFlo III and the ion source of the mass spectrometer for measurement of the sulfur isotope ratio. The reactor and the GC oven were heated stepwise to working temperatures of 1030 and 90°C, respectively. The flow rate of the carrier He was maintained at 80 mL/min and that of O_2 at

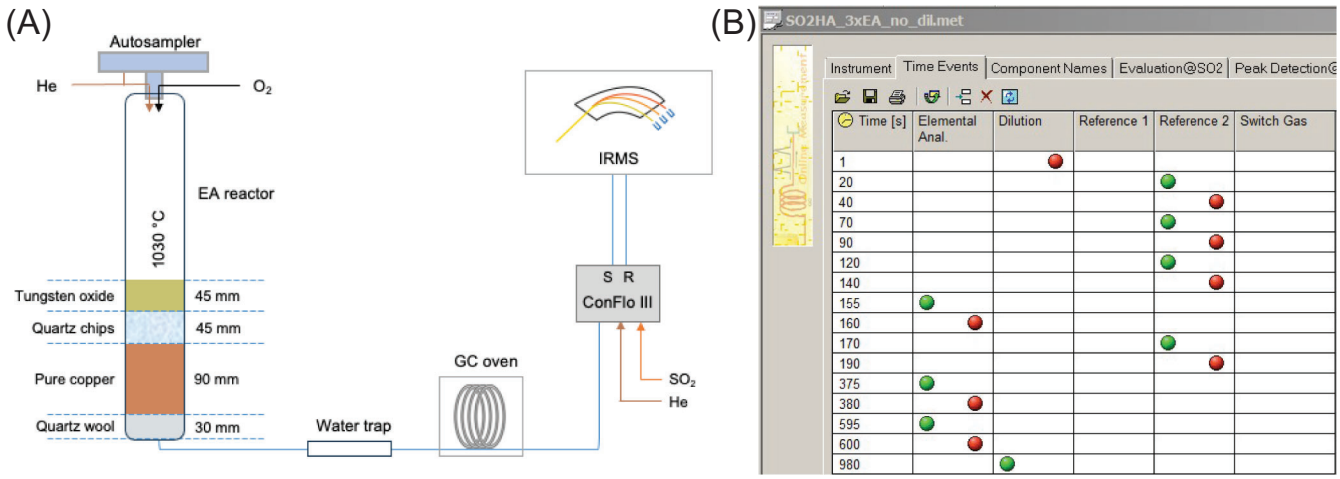

FIGURE 1 Schematic diagram of the elemental analysis/isotope ratio mass spectrometry (EA/IRMS) system with an EA reactor for the sulfur isotope analyses (A). Sequence of the time events (Isodat 3.0) in the 3×EA/IRMS method used to measure sulfur isotopes (B). The total acquisition time was 1000 s. GC, gas chromatography. [Color figure can be viewed at wileyonlinelibrary.com]

30 mL/min. Before starting the analytical sequences for the sulfur isotope analyses, the GC column was conditioned at 98°C for 24 h.

Before the $\delta^{34}S$ analyses, the samples and calibration standards were dried at 50°C for 48 h and stored in an acrylic desiccator cabinet (Nalgene part no. 5317-0070) before use. Aliquots of the calibration standards, international RMs, and samples were weighed in tin capsules for solids (3.3 × 5 mm, part no. SA76980502). Vanadium pentoxide (V_2O_5, ≥98.0%, CAS no. 1314-62-1, part no. SA990709C) was added as an oxidation catalyst in amounts approximately once to twice that of the standard or sample. The optimized O_2 pulse in the EA method was applied for 90 s, and the addition of V_2O_5 to all the capsules ensured that the oxygen available for the combustion of the sulfur-containing samples and calibration and validation standards essentially had the same isotopic composition and remained constant during the analytical sequence; this process improved the reproducibility of the measured $\delta^{34}S$ values.

For example, the sample aliquot sizes were 400–600 µg for barium sulfate ($BaSO_4$), 800–1000 µg for silver sulfide (Ag_2S), 300–600 µg for most relatively pure sulfides (e.g., bornite Cu_5FeS_4, chalcopyrite $CuFeS_2$, cinnabar HgS, galena PbS, pyrite FeS_2, sphalerite ZnS, molybdenite MoS_2, and millerite NiS), and 50–150 µg for elemental sulfur. The tin capsules with standard or sample aliquots were placed in the autosampler and combusted sequentially using the EA/IRMS acquisition methods. The stable isotopic composition of sulfur was reported in the delta (δ) notation as the difference in the molar ratio of the heavy-to-light isotope of sulfur ($^{34}S/^{32}S$) relative to the VCDT standard:

$$\delta^{34}S_{\text{sample/standard}} = \frac{R\left(^{34}S/^{32}S\right)_{\text{sample}}}{R\left(^{34}S/^{32}S\right)_{\text{standard}}} - 1.$$

The δ values were multiplied by 1000 and reported using the milliurey (mUr) unit, as recommended by the International Union of Pure and Applied Chemistry (IUPAC).[24] One mUr is equivalent to one per mil (‰), and this unit is no longer acceptable because it is not an SI unit. The SO_2 standard gas was calibrated against the VCDT scale using the IAEA-S-1 Ag_2S RM with a $\delta^{34}S$ value of −0.3 mUr. No correction was applied for the contribution of $^{18}O/^{16}O$ to $^{34}S/^{32}S$ because the sample and calibration/reference standards produced SO_2 in the same combustion environment with similar excess and source of oxygen (i.e., O_2 gas and V_2O_5).[22] The EA/IRMS system was operated with Isodat 3.0 software (Thermo Fischer Scientific, Bremen, Germany), and the software was used to collect the data and perform the calculations. The SO_2 peak detection and automatic integration were performed using the conventional parameters (i.e., start slope = 0.2, end slope = 0.2, peak minimum high = 50, peak resolution = 20%, maximum peak width = 180, no limit for start and end peak detection, individual background). The measured $\delta^{34}S$ values based on the working gas cylinder of SO_2 were normalized to the VCDT scale using three-point calibration with international RMs and laboratory standards (Table 1). The calibrations were performed using replicate analyses of two sets from the three standards at the beginning and end of the analytical sequences. A drift correction was applied based on a linear function of the differences between the start and end calibrations and the number of acquisition lines between them. The measured $\delta^{34}S$ values were corrected/normalized to the VCDT scale, accounting for the line-specific slope and intercept change. The accuracy and analytical precision of the $\delta^{34}S_{\text{sample/VCDT}}$ values were assessed using replicate analyses of the RM not used for calibration. The reproducibility of the EA/IRMS $\delta^{34}S$ values was better than ±0.3 mUr. The EA reactor was replaced, and the GC column was reconditioned when the SD of the $\delta^{34}S$ values corrected with the first-, end-, and drift-calibration equations was >0.2 mUr. At that point, the EA had generally between 150 to 200 combustions, depending on the size of the sample aliquots and the amount of V_2O_5 added.

2.3 | The 3×EA/IRMS acquisition method for δ ^{34}S analysis

The 3×EA/IRMS method for sulfur isotope analyses used the same elemental analyzer conditions as those described previously (Section 2.2); these conditions included the reactor packing, reactor and GC temperatures of 1030 and 90°C, respectively, and the flow rates of 80 mL/min for the carrier He and 30 mL/min for oxygen. After the SO_2 peak was centered at *m/z* 64, the time events in the acquisition method included the following: injection into the He carrier gas of four SO_2 reference gas pulses at 20–40, 70–90, 120–140, and 170–190 s; three activations of the elemental analyzer at 155–160, 375–380, and 595–600 s; no He dilution until 980 s; and a total time of 1000 s (Figure 1B). The He dilution was turned on during the last 20 s to help decrease the build-up of the residual SO_2 within the capillary to the ion source; additionally, this reduced the SO_2 background signals before the appearance of the analyte gases from the subsequent acquisition. Reconditioning the GC column every 48 h for 1 h at 98°C was necessary to ensure good shape and separation of the SO_2 peaks in the 3×EA/IRMS outputs (Figure 2).

When sufficient material was available, all samples and calibration standards were measured in triplicate using the 3×EA/IRMS method. Each acquisition sequence included the first and last lines of blanks (first line with no capsule in the first EA cycle and empty capsules in

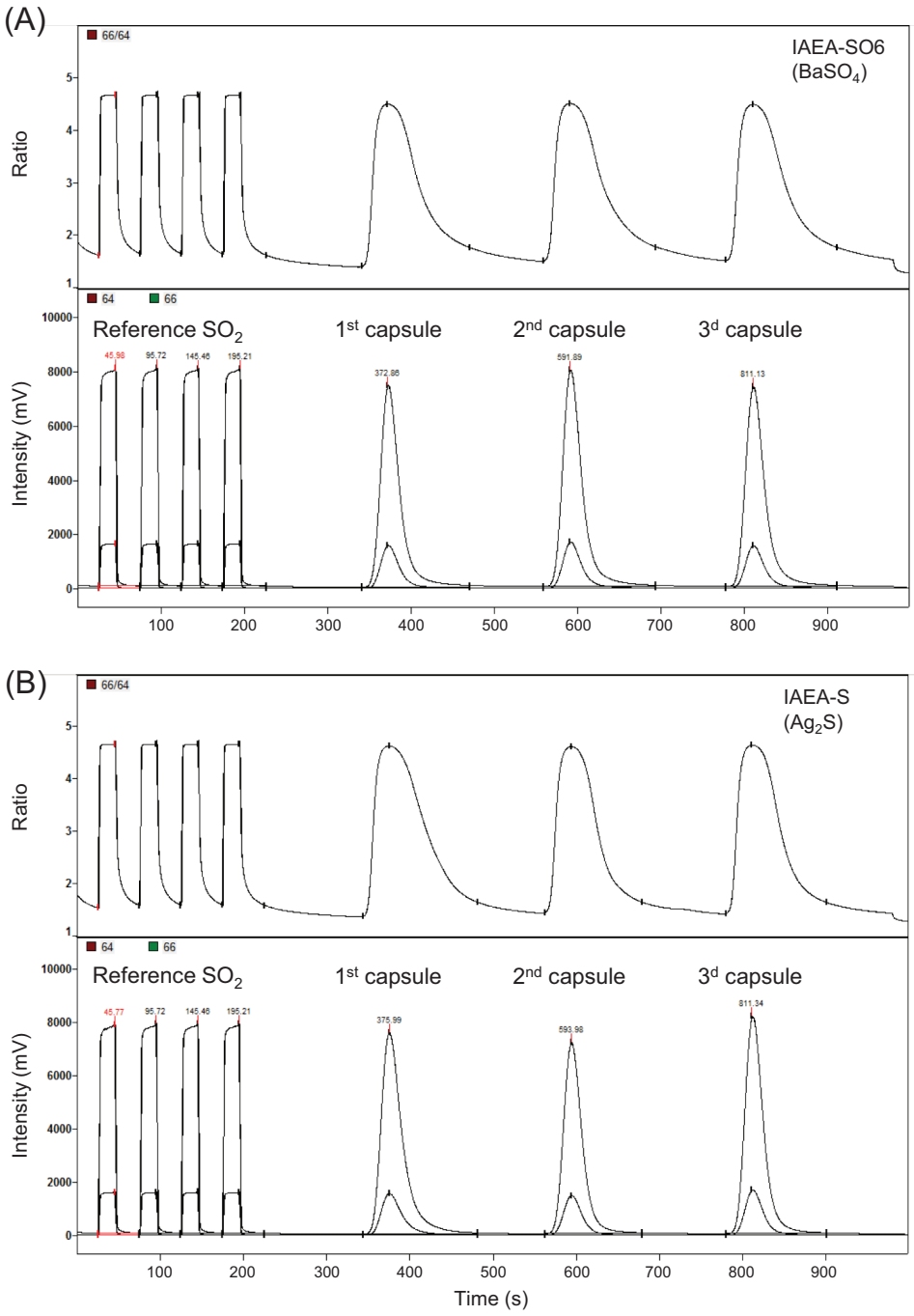

FIGURE 2 Typical 3× elemental analysis/isotope ratio mass spectrometry (EA/IRMS) chromatograms for the sulfur isotope analyses of sulfate (A) and sulfide (B) samples. The *m/z* 64 and 66 traces represent ions of the SO_2 reference gas (four rectangular peaks), respectively, followed by peaks from the SO_2 liberated by three consecutive combustions of tin capsules containing aliquots of the same material or blank samples. [Color figure can be viewed at wileyonlinelibrary.com]

the following two cycles with an inverted capsule order for the last line), 6 lines of calibration standards (3 at the start and end of the analytical sequence, with each line for three combustion reactions of the same standard), and 20 lines (each with three EA cycles) for the samples; these 20 lines were analyzed between the blank and calibration lines. Depending mainly on the amount of sample available for $\delta^{34}S$ analysis, the three combustion reactions per acquisition line included three capsules with the same material (as in the case of calibration standards), or an empty capsule in the first EA cycle and capsules containing sample aliquots in the following two cycles. This last order of the capsule combustion was also applied in the first sample line after the set of calibration standards to minimize the memory effect that could occur due to the consecutive combustion of materials with different $\delta^{34}S$ values (e.g., sulfate calibration standards, −34.08 and 21.12 mUr in IAEA-SO-6 and NBS 127, respectively; sulfide calibration standards, −34.49 and 22.62 mUr in IAEA-S-3 and IAEA-S-2, respectively). Additionally, in cases where the sample had a minimal amount of material available or, particularly important, was a quality control standard (i.e., IAEA-S-1, −0.3 mUr), the capsule containing the analyte was set between two blanks (empty capsules).

The calibration and quality control standards (Table 1), normalization, and drift correction of the 3×EA/IRMS $\delta^{34}S$ values were essentially the same as described for conventional EA/IRMS in Section 2.2; for the drift correction function, the number of lines between the start and end calibration standards set was replaced by the number of combustions.

Finally, the conventional EA/IRMS method routinely used at the UNIL for sulfur isotope ratio acquisition requires 640 s for a single EA cycle and provides one $\delta^{34}S$ value. The optimized 3×EA/IRMS-$\delta^{34}S$ method with three EA cycles can provide three $\delta^{34}S$ values in 1000 s, which can be used for blanks, calibration or quality control standards, and samples. The 3×EA/IRMS-$\delta^{34}S$ method requires approximately 333 s per sample, reducing the analysis time and energy consumption and the He, O_2, and SO_2 reference gases by approximately 50% compared to the conventional method.

2.4 | Method for purging gas tubing after SO_2 usage

Here, we describe the connection of the SO_2 reference gas cylinder before entering the ConFlo III interface of the EA/IRMS system and a procedure for purging the gas line using an N_2 flushing system after SO_2 usage to prolong the lifetime of the ConFlo valves and pressure regulator. This method can also be used in conjunction with any CNS EA/IRMS system.

All gas bottles and fittings for special gases were within well-ventilated compressed gas cylinder cabinets. The fittings for the corrosive gases, custom-prepared for SO_2 bottles, were provided by Carbagas/Multigas (Domdidier, Switzerland) and are depicted in Figure 3. The assembled fittings included a pressure reducer with a metal diaphragm BS.S 0.2–4 bar (BS stands for bellow-soufflet and S for 316L stainless steel, hereafter SS) and polytrifluorochloroethylene (PTFCE) and PTFE seals (Carbagas part no. 15951), an SV10 safety relief valve of 316L SS and FPM 358 (part no. 155253), an adapter G3/8″-16 × 1.336 SI (part no. 16506), a bottle connection G5/8″R of SS (for SO_2) (part no. 16356), compression fitting Gyrolok, G3/8″-1/4″ of SS (part no. 16566), and a high-pressure flushing system (part no. 72557). The flushing system combined the valves and connections between the SO_2 gas cylinder and the pressure reducer (Figure 3); this setup enabled the purging of the system with pure N_2 (99.999% purity). The flushing N_2 gas was connected to an 316L SS high-purity,

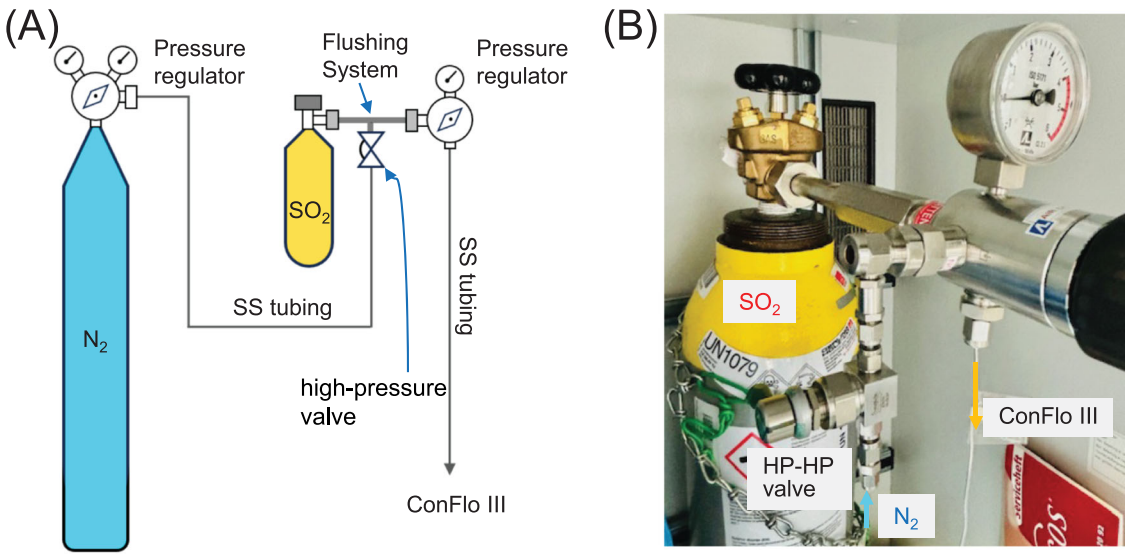

FIGURE 3 Schematic diagram of the SO_2 reference gas connections before entering the ConFlo III of the elemental analysis/isotope ratio mass spectrometry (EA/IRMS) system (A). Pure N_2 gas was used to purge the residual gas in the pressure regulator attached to the SO_2 gas cylinder (B) until ConFlo III (reference open split) was reached after the batch of analytical sequences of the $\delta^{34}S$ analyses was finished. SS, stainless steel. [Color figure can be viewed at wileyonlinelibrary.com]

high-pressure diaphragm-sealed valve (Swagelock part no. 679791 SS-DLS4; provided by Arbor Fluidtec AG, Niederrohrdorf, Switzerland). When the valve was open, N_2 exited from the 50 L gas cylinder with an outlet pressure of 2–3 bar through the system, and the residual SO_2 was purged through the pressure regulator, connections, and tubing to the open split in the ConFlo III. After several cycles of increasing the N_2 pressure in the space between the SO_2 cylinder and the pressure reducer and releasing it, the mixture was flushed with N_2 at approximately 2 bar through all the connections between the SO_2 gas bottle and the ConFlo III for 48 h. The pressure regulator and pressure gauge in the ConFlo inlet for SO_2 were made mainly from SS and Viton (Parker-Porter Precision regulator part no. and pressure gauge part no. RCH40-3 0 to 2.5 bar; both from PKM SA, Lyss, Switzerland). During the sulfur isotope analytical sequences, the ConFlo III was warmed using an Osram SICCATHERM IR 1, 250 W 240 V heat lamp. The pure N_2 purging method of the residual gases in the lines of the EA/IRMS interface provides a low-cost, work-effective, and efficient procedure to prolong the lifetime of the valves and pressure regulators and minimizes the risk of blockage of the SS or fused silica capillaries.

2.5 | Application example: 3×EA/IRMS $\delta^{34}S$ measurement of AVS and CRS samples

First, we described the setup used for the simultaneous four-sample extraction of the AVS and CRS in Lake Joux sediments and Minas Gerais black shale. The multiple-port apparatus was modified from the reactor system used by Canfield et al.[25] to release the pyrite-bound sulfur using treatment with a hot acidic chromium (II) chloride ($CrCl_2$) solution. Some modifications were described previously.[26–28] At UNIL, the experimental apparatus for AVS and CRS extraction was installed within a well-ventilated 1500 mm wide fume hood (Waldner Laboreinrichtungen GmbH & Co.KG, Wangen, Germany) and was built using commercially available parts (Figure 4). The setup was designed to be easily installed and removed from the fume hood. Once the researcher has finished using the chromium-reduction apparatus, it could be quickly dissembled and stored in a box, leaving the fume hood free for other laboratory activities.

The main parts included a heating mantle, a borosilicate two-neck 250 mL RBF (hereafter called the reaction flask), and a multiple adapter with two parallel necks (both from VWR International AG, Dietikon, Switzerland, part nos. 271-1407 and 201-2216), a condenser, a 50 mL RBF for gas washing, a 50 mL RBF for reduced sulfur trapping, an injection port made from a PTFE straight-through two-way stopcock (6 mm external diameter), and various conical stoppers of natural rubber with one or two (custom-made) holes (Figure 4A). A distribution block (manifold block) connected to a pressure regulator attached to an N_2 gas cylinder (99.999% purity; Air Liquide/Carbagas, Lausanne, Switzerland) provided N_2 to the four reactors (Figure 4B). Each outlet had a manual pressure relief PTFE valve (Semadeni AG, Ostermundigen, Switzerland, part no. 4141), allowing independent control of the N_2 flow in each reactor. N_2 was applied through a polyvinyl chloride (PVC) plastic tube (100 mm length, 8 mm ID, 10 mm OD) connected to a glass tube (300 cm length, 2 mm ID, 6 mm OD) inserted in the vertical neck of the reaction flask to a depth of up to 5 mm from the bottom. This position allowed continuous bubbling of N_2 into the reaction solutions. The condenser (top) outlet was connected using PTFE capillaries to the wash RBF and the sulfur trap RBF. The condenser-to-washing-RBF PTFE transfer line (150 cm length, 4 mm ID, 5 mm OD from Semadeni AG, Ostermundigen, Switzerland; part no. 7562) had one end connected to an 8 cm long glass tube and the other to a 12 cm long glass tube (both with 4 mm ID and 5 mm OD). The rubber

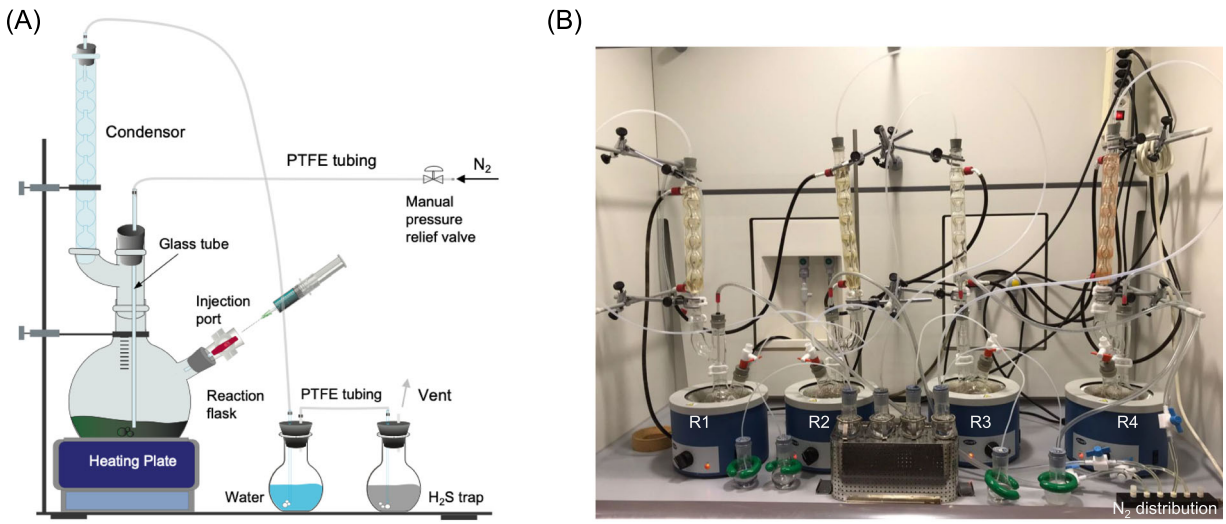

FIGURE 4 Schematic of the apparatus used for extraction of acid-volatile sulfur (AVS) and chromium-reducible sulfur (CRS) at Institute of Earth Surface Dynamics-University of Lausanne (IDYST-UNIL) (A). Photograph of the experimental setup, consisting of four independent reactors (R1, R2, R3, and R4), which allows simultaneous extraction of different samples working with distinct N_2 gas flows, temperatures, and reaction times (B). PTFE, polytetrafluoroethylene. [Color figure can be viewed at wileyonlinelibrary.com]

stoppers on the condenser outlet and the vertical neck of the reaction flask had one hole. An 8 cm long glass tube was inserted through the rubber stopper on the condenser until approximately 2 cm was inside. Two small holes were carefully drilled on the rubber stoppers of the washing and trapping RBFs. A 12 cm glass tube was inserted into one hole of the rubber stopper on the washing RBF to a depth of up to 2–4 mm from the bottom (Figure 4A). One end of the washing RBF-to-H_2S-trapp PTFE transfer line (50 cm length, 2 mm ID, 3 mm OD from Semadeni, part no. 7559) was inserted in the second hole until 10 mm passed across the rubber stopper into the washing RBF. The other end of the PTFE tube was inserted in one hole of the rubber stopper on the reduced sulfur trap to a depth of up to 2–4 mm from the bottom of the RBF. A conical tube was obtained by heating and stretching a glass tube (40 mm length, 4 mm ID, 5 mm OD), and the tube had an end with a 2 mm ID. This tighter part was inserted in the second hole of the reduced sulfur trap rubber stopper to pass across 5 mm and functioned as the N_2 vent. Leak-free connections of PTFE tubing–glass tubes and insertions of the capillaries in rubber stoppers were obtained with all-purpose glue (details in Spangenberg et al.[22]). The outlet of the 40 mm glass tube on the reduced sulfur trap was vented. All the glassware connections were ensured with PTFE clamps, and the sulfur traps were stabilized with weight rings (Figure 4B).

Briefly, the following experimental manipulations were necessary for the AVS and CRS extractions. An aliquot of the sample powder (generally 0.5–3 g) was introduced into the reaction flask and covered with 2–5 mL ethanol to allow disaggregation of the material and release the air trapped in the particles. Then, 25 mL of MQW was added to the gas-washing RBFs, and 25 mL of a 0.2 M zinc acetate solution was added to the sulfur trapping RBFs. The injection ports were closed, and all glassware connections were checked for leaks before the system was flushed with N_2 for 15 min. During this time, the N_2 flow was increased to allow bubbling of the sample–ethanol slurry and the washing and sulfur trapping solutions. This process created an oxygen-free atmosphere before the chemical extraction started. Under the continuous flow of N_2 at a rate of 2–3 bubbles/s in the reduced sulfur trap, 20 mL of 6 N HCl was injected into the reaction flask through the injection port using a 60 mL plastic syringe to start the reaction, and the reaction was allowed to proceed at room temperature for 2 h. During the reaction time, the AVS produced was continuously carried by the N_2 flow and trapped in the sulfur trapping solution as zinc sulfide (ZnS) through a reaction with the zinc acetate solution. The trapping solutions were then replaced by new ones and after 15 min of continuous N_2 flushing, the extraction of CRS was started with the injection 30 mL of a 1.0 M $CrCl_2$ solution in the reaction flask with a 60 mL plastic syringe. The reaction flask was heated, and the cooling water flow through the condenser was controlled such that most of the liquid phases in the steam were returned to the reaction flask. The mixture was allowed to boil for 2 h under a continuous flow of N_2 at a rate of 2–3 bubbles/s in the new sulfur trap. N_2 carried the released H_2S (mainly from pyrite) to the washing RBF and then to the sulfur trap; here it was converted to ZnS. The ZnS from AVS and CRS was converted to Ag_2S by adding $AgNO_3$ to the ZnS-containing trapping solutions; these solutions were subsequently stored at room temperature in the dark for at least 48 h. The Ag_2S precipitate was filtered through a 0.2 µm nitrocellulose filter, rinsed with 5% ammonia solution and MQW, and dried at 40°C for 48 h before isotopic analysis. Between the sample batches, the AVS and CRS extraction apparatus was disassembled, and the reaction, washing, and trapping flasks were changed for a second set of glassware, which was previously washed, rinsed, and dried. The PTFE capillaries were checked for possible blocking, removed if necessary, cleaned with deionized water, rinsed with MQ water, and dried with compressed air.[22] The analytical setup described above was previously validated with UNIL laboratory standard pyrite (Table 1) and used for the extraction of CRS from rocks with a wide range of ages, including (a) pyrite from fossils, concretions, and host sediments in the 2.1 Ga Paleoproterozoic sedimentary succession of Gabon (Ossa-Ossa et al., unpublished data); (b) samples of limestone-dolomite rhythmites from the Precambrian Polanco Formation in Uruguay (Gaucher et al., unpublished data); and more recently, the CRS-pyrite obtained from the insoluble residue following the carbonate-associated sulfur (CAS) extraction in samples across the Smithian-Spathian boundary from Qiakong, South China.[29] In all these studies, sulfur isotope analyses of the CRS-derived Ag_2S samples were performed with the conventional EA/IRMS routinely used at the UNIL (Section 2.2). For the first time, the $\delta^{34}S$ values of samples with limited material availability, such as precious samples, including Ag_2S from the AVS and CRS-pyrite extracted from Lake Joux sediments and black shale samples from the Rio das Velhas greenstone belt, were determined with 3×EA/IRMS.

3 | RESULTS AND DISCUSSION

3.1 | Validation of the analysis of $\delta^{34}S$ using 3×EA/IRMS

Typical outputs of the 3×EA/IRMS method for sulfur isotope analyses of sulfates (e.g., $BaSO_4$ IAEA-SO-6) and sulfides (e.g., Ag_2S IAEA-SI) are depicted in Figure 2. The retention times of the SO_2 peaks from the three capsules were approximately 376, 594, and 811 s. No appreciable increases or changes in the backgrounds of the *m/z* 64 and 66 traces or 66/64 ratios were observed, suggesting no appreciable (or very limited) carryover of residual SO_2 from previous combustion reactions. Blanks, RMs, and laboratory standards were further scrutinized, and the results confirmed the apparent lack of memory effect. Different blank 3×EA/IRMS analyses were considered: three combustion reactions with no tin capsules, three with empty tin capsules, and three with tin capsules containing 500–5000 µg V_2O_5. The blanks without capsules showed no changes in the background for the *m/z* traces or ratios. The other blanks showed only some background increase in the number of times the SO_2 peaks eluted. However, they did not yield a detectable peak with the conventional peak detection parameters in Isodat 3.0 software (Section 2.2). Manually optimized definitions of the peak and

background generated the $\delta^{34}S$ values within ±0.05 mUr deviation from those obtained automatically.

Nine RM_S and four sulfate and sulfide laboratory standards, covering a wide range of $\delta^{34}S$ values, between −34.05 and +22.62 mUr, were used to validate the 3×EA/IRMS method (Table 1). The $BaSO_4$ standards included the RMs NBS 127, IAEA-SO-5, IAEA-SO-6, and the synthetic $BaSO_4$ UVA sulfate and Fx-sulfate. The standards used to normalize the measured $\delta^{34}S$ values for elemental sulfur and transition metal sulfides included elemental sulfur IAEA-S-4, silver sulfides IAEA-S-1, S-2, and S-3, and zinc sulfides NBS-122 and NBS-123. The laboratory sulfide standards were UNIL-PyE (pyrite, FeS_2) and UNIL-Cin (synthetic mercury sulfide, cinnabar, HgS). The accepted $\delta^{34}S$ values for the standards are given in Table 1.

The $\delta^{34}S$ values of the RMs and laboratory standards determined using conventional EA/IRMS and 3×EA/IRMS are summarized in Table 1. The results are reported as the means for replicate analyses (n = 6–12) with the SD. Both sets of measurements provided values that were highly correlated with the recommended values and with each other (Figure 5). In Table 1, the 3×EA/IRMS results are presented in two columns: one column gives the average ±1 SD from the $\delta^{34}S$ values derived from the three combustion reactions per acquisition in the analytical (method) replicates, and the other column shows the average ±1 SD only from the second and third combustion reactions. This approach would help avoid potential memory/carryover effects from the previous EA combustion reactions of a different material. The SDs are estimates of the intermediate precisions (repeatability and reproducibility) of the $\delta^{34}S$ measurements. A comparison of the average ±1 SD of the uncertainties in $\delta^{34}S$ for all RMs and laboratory standards measured using the different EA/IRMS methods (0.212 ± 0.061 mUr for conventional EA/IRMS, 0.261 ± 0.086 mUr for the three $\delta^{34}S$ values from 3×EA/IRMS, and 0.168 ± 0.066 mUr for the second and third $\delta^{34}S$ values from 3×EA/IRMS) provided precisions similar (*P*-values between 0.7 and 0.8) to those for the accepted values of the standards (0.169 ± 0.065 mUr).

The agreement between the mean values obtained from RMs and laboratory standards and the recommended $\delta^{34}S$ values provided a measure of the accuracy of the different methods (Table 1; Figure 5). Comparisons between the means for each group (i.e., EA/IRMS methods) from replicate $\delta^{34}S$ analyses of RMs and laboratory standards were performed using paired-samples *t*-test. This approach provides a simple way to compare the quality of the different methods. The means of the three $\delta^{34}S$ values from the 3×EA/IRMS acquisitions and the means of only the second and third $\delta^{34}S$ values did not significantly differ from those obtained using conventional EA/IRMS with a single combustion reaction (*P*-values between 0.1 and 1.0).

Additionally, the developed 3×EA/IRMS-$\delta^{34}S$ procedure was applied during the last few months for analyses of a wide variety of sulfide samples from students and colleagues studying the geochemistry of ore deposits. The analyzed sulfide minerals included, among others, bornite (Cu_5FeS_4), chalcopyrite ($CuFeS_2$), galena (PbS), molybdenite (MoS^2), pyrite (FeS_2), pyrrhotine ($Fe_{1-x}S$), and sphalerite (ZnS). The values obtained using 3×EA/IRMS were in good agreement with those obtained using conventional EA/IRMS within an analytical error of ±0.3 mUr.

In summary, the 3×EA/IRMS-$\delta^{34}S$ method reduced He, energy, and SO_2 reference gas use and instrumental time by approximately 50% compared to the conventional EA/IRMS for sulfur isotope analyses. These reductions had an immediate impact on the cost of analysis and decreased the turnaround time for sulfur isotope analyses. The accuracy and precision of the $\delta^{34}S$ measurements made using 3×EA/IRMS were similar to or potentially better than those of conventional EA/IRMS.

3.2 | Example of 3×EA/IRMS for $\delta^{34}S$ analysis of AVS and CRS-pyrite

The $\delta^{34}S$ values of AVS extracted from Lake Joux sediments (from 1 to 28 cm deep, Table 2) ranged between 1.63 ± 0.12 and 4.03 ± 0.1 mUr, whereas the CRS-pyrite ranged between 1.17 ± 0.32 and 6.39 ± 0.21 mUr (Table 2). As expected, no AVS was released from the deepest sediment sample. The positive and similar $\delta^{34}S$ values of

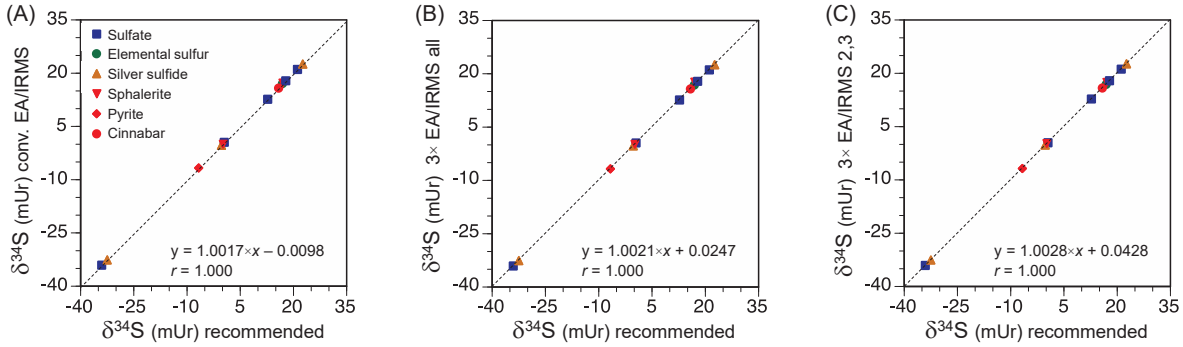

FIGURE 5 Sulfur isotope ratios in reference materials and laboratory standards using conventional elemental analysis/isotope ratio mass spectrometry (EA/IRMS) (A), 3×EA/IRMS considering the three values of each acquisition (B), and 3×EA/IRMS considering the second and third values of each acquisition (C) compared with the recommended values. The number of replicates and uncertainties are given in Table 1. [Color figure can be viewed at wileyonlinelibrary.com]

TABLE 2 Sulfur isotope composition of the acid-volatile sulfur (AVS) and chromium-reducible sulfur (CRS) extracts from rocks and sediments obtained using 3× elemental analysis/isotope ratio mass spectrometry (EA/IRMS).

		Ag_2S from AVS		Ag_2S from CRS	
Identifier	Description	$\delta^{34}S_{VCDT}$ (mUr)	Uncertainty[a]	$\delta^{34}S_{VCDT}$ (mUr)	Uncertainty[a]
LJ-1–3	Sediment	2.03	0.12	4.89	0.08
LJ-4–6	Sediment	4.03	0.10	3.35	0.10
LJ-8–10	Sediment	3.78	0.08	2.87	0.11
LJ-12–14	Sediment	1.63	0.12	1.35	0.25
LJ-22–24	Sediment	3.90	0.17	6.39	0.21
LJ-26–28	Sediment	-	-	1.17	0.32
RDV-A	Black shale	-	-	4.09	0.02
RDV-B	Black shale	-	-	4.16	0.02
RDV-C	Black shale	-	-	4.78	0.09
RDV-D	Black shale	-	-	4.63	0.08
RDV-E	Black shale	-	-	4.52	0.03
RDV-F	Black shale	-	-	3.66	0.06

Abbreviations: -, not analyzed; LJ, Lake Joux (Switzerland); RDV, Rio das Velhas greenstone belt (Brazil).
[a]Uncertainties correspond to one standard deviation of three measurements.

the AVS and CRS-pyrite from Lake Joux reflected a diagenetic process in an environment with low sulfate levels (42 μM) and elevated organic matter content (averaging 10 wt% total organic carbon, as yet unpublished). No AVS was recovered from the Archean RDV black shale; the $\delta^{34}S$ values of the CRS-pyrite covered a narrow range from 4.09 to 4.89 mUr (Table 2). These relatively uniform values suggest environmental stability characterized by limited sulfate levels during the deposition of the black shales.[23,30,31]

4 | CONCLUSIONS

The proposed 3×EA/IRMS method using three combustion cycles in a single analytical acquisition provides accurate and precise sulfur isotope compositions of sulfate and sulfide samples while saving approximately 50% of He, energy, SO_2 reference gas, O_2, and analysis time and cost compared to those of conventional EA/IRMS. If the combustion reactions in all three EA cycles involve the same material, standard, or sample, the derived second and third $\delta^{34}S$ values were not affected by any carryover or memory effects. The 3×EA/IRMS method is particularly efficient when sample analyses require replicate analyses and may be strategically beneficial for $\delta^{34}S$ measurements of small amounts of precious samples, such as Ag_2S from AVS and CRS or $BaSO_4$ from carbonate-associated sulfate; with these samples, the material can be combusted between two blanks.

ACKNOWLEDGMENTS

The stable isotope facilities at the Institute of Earth Surface Dynamics (IDYST) are supported by the Faculty of Environmental Geosciences of the University of Lausanne and the Swiss National Science Foundation. Jorge E. Spangenberg would like to thank Elise Ödegaard and Filipe Santos Antunes for laboratory assistance. Alice Bosco-Santos would like to thank Foundation Agassiz for the financial support, Jasmine Berg for support with Lake Joux fieldwork, Virgil Pasquier for discussions on the interpretation of Lake Joux $\delta^{34}S$ values, and William Gilhooly for support with Rio das Velhas fieldwork and data interpretation. Eva E. Stüeken and an anonymous reviewer are thanked for their constructive comments and Dr. Roland Bol for editorial handling of the manuscript.

AUTHOR CONTRIBUTIONS

Jorge E. Spangenberg: Conceptualization; data curation; formal analysis; methodology; writing - original draft; writing - review and editing; visualization. **Alice Bosco-Santos:** Data curation; formal analysis; writing - review and editing.

PEER REVIEW

The peer review history for this article is available at https://www.webofscience.com/api/gateway/wos/peer-review/10.1002/rcm.9866.

DATA AVAILABILITY STATEMENT

The data that support the findings of this study are available from the corresponding author upon reasonable request.

ORCID

Jorge E. Spangenberg https://orcid.org/0000-0001-8636-6414
Alice Bosco-Santos https://orcid.org/0000-0002-7357-8781

REFERENCES

1. Glowacki BA, Nuttall WJ, Clarke RH. Beyond the helium conundrum. *IEEE Trans Appl Supercond*. 2013;23(3):0500113. doi:10.1109/TASC.2013.2244633
2. Halperin WA. The impact of helium shortages on basic research. *Nat Phys*. 2014;10(7):467-470. doi:10.1038/nphys3018
3. Kramer D. Helium prices surge to record levels as shortage continues. *Phys Today*. 2023;76(9):18-20. doi:10.1063/PT.3.5305

4. Siddhantakar A, Santillán-Saldivar J, Kippes T, Sonnemann G, Reller A, Young SB. Helium resource global supply and demand: geopolitical supply risk analysis. *Resour Conserv Recycl*. 2023;193:106935. doi:10.1016/j.resconrec.2023.106935
5. Abas N, Kalair A, Khan N. Review of fossil fuels and future energy technologies. *Futures*. 2015;69:31-49. doi:10.1016/j.futures.2015.03.003
6. Mišík M. The EU needs to improve its external energy security. *Energy Policy*. 2022;165:112930. doi:10.1016/j.enpol.2022.112930
7. Spangenberg JE. Three combustion reactions in a single elemental analysis and isotope ratio mass spectrometry acquisition as a strategy to save helium and energy. *Rapid Commun Mass Spectrom*. 2024;38(1):e9663. doi:10.1002/rcm.9663
8. Canfield DE. The evolution of the earth surface sulfur reservoir. *Am J Sci*. 2004;304(10):839-861. doi:10.2475/ajs.304.10.839
9. Seal RR. Sulfur isotope geochemistry of sulfide minerals. *Rev Mineral Geochem*. 2006;61(1):633-677. doi:10.2138/rmg.2006.61.12
10. Stüeken EE, Catling DC, Buick R. Contributions to late Archaean sulphur cycling by life on land. *Nat Geosci*. 2012;5(10):722-725. doi:10.1038/NGEO1585
11. Fike DA, Bradley AS, Rose CV. Rethinking the ancient sulfur cycle. *Annu Rev Earth Planet Sci*. 2015;43(1):593-622. doi:10.1146/annurev-earth-060313-054802
12. Mateos K, Chappell G, Klos A, et al. The evolution and spread of sulfur cycling enzymes reflect the redox state of the early earth. *Sci Adv*. 2023;9(27):eade4847. doi:10.1126/sciadv.ade4847
13. Burke A, Present TM, Paris G, et al. Sulfur isotopes in rivers: insights into global weathering budgets, pyrite oxidation, and the modern sulfur cycle. *Earth Planet Sci Lett*. 2018;496:168-177. doi:10.1016/j.epsl.2018.05.022
14. Jørgensen BB, Findlay AJ, Pellerin A. The biogeochemical sulfur cycle of marine sediments. *Front Microbiol*. 2019;10:849. doi:10.3389/fmicb.2019.00849
15. Li JL, Schwarzenbach EM, John T, et al. Uncovering and quantifying the subduction zone sulfur cycle from the slab perspective. *Nat Commun*. 2020;11(1):514. doi:10.1038/s41467-019-14110-4
16. Giesemann A, Jaeger HJ, Norman AL, Krouse HP, Brand WA. Online sulfur-isotope determination using an elemental analyzer coupled to a mass-spectrometer. *Anal Chem*. 1994;66(18):2816-2819. doi:10.1021/ac00090a005
17. Grassineau NV, Mattey DP, Lowry D. Sulfur isotope analysis of sulfide and sulfate minerals by continuous flow-isotope ratio mass spectrometry. *Anal Chem*. 2001;73(2):220-225. doi:10.1021/ac000550f
18. Craddock PR, Rouxel OJ, Ball LA, Bach W. Sulfur isotope measurement of sulfate and sulfide by high-resolution MC-ICP-MS. *Chem Geol*. 2008;253(3–4):102-113. doi:10.1016/j.chemgeo.2008.04.017
19. Pribil MJ, Ridley WI, Emsbo P. Sulfate and sulfide sulfur isotopes ($\delta^{34}S$ and $\delta^{33}S$) measured by solution and laser ablation MC-ICP-MS: an enhanced approach using external correction. *Chem Geol*. 2015;412:99-106. doi:10.1016/j.chemgeo.2015.07.014
20. Spangenberg JE, Zufferey V. Carbon isotope compositions of whole wine, wine solid residue, and wine ethanol, determined by EA/IRMS and GC/C/IRMS, can record the vine water status—a comparative reappraisal. *Anal Bioanal Chem*. 2019;411(10):2031-2043. doi:10.1007/s00216-019-01625-4
21. Brand WA, Coplen TB, Vogl J, Rosner M, Prohaska T. Assessment of international reference materials for isotope-ratio analysis (IUPAC technical report). *Pure Appl Chem*. 2014;86(3):425-467. doi:10.1515/pac-2013-1023
22. Spangenberg JE, Saintilan NJ, Palinkas SS. Safe, accurate, and precise sulfur isotope analyses of arsenides, sulfarsenides, and arsenic and mercury sulfides by conversion to barium sulfate before EA/IRMS. *Anal Bioanal Chem*. 2022;414(6):2163-2179. doi:10.1007/s00216-021-03854-y
23. Bosco-Santos A, Gilhooly WP III, de Melo-Silva P, et al. Neoarchean atmospheric chemistry and the preservation of S-MIF in sediments from the São Francisco Craton. *Geosci Front*. 2022;13(5):101250. doi:10.1016/j.gsf.2021.101250
24. Brand WA, Coplen TB. Stable isotope deltas: tiny, yet robust signatures in nature. *Isotopes Environ Health Stud*. 2012;48(3):393-409. doi:10.1080/10256016.2012.666977
25. Canfield DE, Raiswell R, Westrich JT, Reaves CM, Berner RA. The use of chromium reduction in the analysis of reduced inorganic sulfur in sediments and shales. *Chem Geol*. 1986;54(1–2):149-155. doi:10.1016/0009-2541(86)90078-1
26. Wotte T, Strauss H, Fugmann A, Garbe-Schönberg D. Paired $\delta^{34}S$ data from carbonate-associated sulfate and chromium-reducible sulfur across the traditional Lower–Middle Cambrian boundary of W-Gondwana. *Geochim Cosmochim Acta*. 2012;85:228-253. doi:10.1016/j.gca.2012.02.013
27. Muller É, Ader M, Chaduteau C, Cartigny P, Baton F, Philippot P. The use of chromium reduction in the analysis of organic carbon and inorganic sulfur isotope compositions in Archean rocks. *Chem Geol*. 2017;457:68-74. doi:10.1016/j.chemgeo.2017.03.014
28. Stebbins A, Algeo TJ, Olsen C, Sano H, Rowe H, Hannigan R. Sulfur-isotope evidence for recovery of seawater sulfate concentrations from a PTB minimum by the Smithian-Spathian transition. *Earth-Sci Rev*. 2019;195:83-95. doi:10.1016/j.earscirev.2018.08.010
29. Edward O, Spangenberg JE, Leu M, et al. Olenekian sulfur isotope records: deciphering global trends, links to marine redox changes and faunal evolution. *Chem Geol*. 2024;649:121984. doi:10.1016/j.chemgeo.2024.121984
30. Canfield DE, Habicht KS, Thamdrup BO. The Archean sulfur cycle and the early history of atmospheric oxygen. *Science*. 2000;288(5466):658-661. doi:10.1126/science.288.5466.658
31. Habicht KS, Gade M, Thamdrup B, Berg P, Canfield DE. Calibration of sulfate levels in the Archean ocean. *Science*. 2002;298(5602):2372-2374. doi:10.1126/science.1078265

How to cite this article: Spangenberg JE, Bosco-Santos A. Sulfur isotope analyses using 3× elemental analysis/isotope ratio mass spectrometry: Saving helium and energy while reducing analytical time and costs. *Rapid Commun Mass Spectrom*. 2024;38(19):e9866. doi:10.1002/rcm.9866